CALCULATING SECOND ORDER SENSITIVITY COEFFICIENTS FOR AIRPORT EMISSIONS IN THE CONTINENTAL U.S. USING CMAQ-HDDM

BY

CALVIN ANTHONY ARTER

February, 2017

Institute for the Environment

University of North Carolina Chapel Hill

Degree Status:

Ph.D. Student

Research Advisor:

Saravanan Arunachalam, Ph.D.

Contents

List of Figures

List of Tables

Abstract

We present higher order sensitivity coefficient calculations for O_3 and $PM_{2.5}$ formation with respect to aircraft emissions in the continental United States, showing the importance of including second order sensitivity coefficients when utilizing sensitivity analyses methods for understanding the impacts of aviation emissions. We designated NO_X and VOC emissions as sensitivity parameters for O_3 formation; and NO_X, SO_2, VOC, EC, OC, and SO_4 emissions as sensitivity parameters for $PM_{2.5}$ formation. The Community Multiscale Air Quality Model (CMAQ) was used to estimate the concentrations and sensitivities of air pollutants in 36×36 km grid cells across the continental United States. First order sensitivity coefficients were calculated for all sensitivity parameters while second order sensitivity coefficients were calculated for only NO_X, VOC, and SO_2 emissions. With the inclusion of second order sensitivity coefficients we are able to show regions of chemical regime (NO_X-limited versus NO_X-inhibited) change in the case of O_3 formation and areas where oxidant limiting indirect effects are important in the case of $PM_{2.5}$ formation. Overall, we find that NO_X emissions are the largest source of nonlinear behavior exhibited in our system. This nonlinear behavior can have an impact on the tropospheric chemistry governing O_3 and $PM_{2.5}$ formation and must be considered when trying to understand how aircraft emissions may impact air quality. We present an analysis utilizing these sensitivity coefficients to estimate the emission reduction needed in five airport grid cells to bring hypothetical regions in $PM_{2.5}$ nonattainment into attainment. Utilizing first order sensitivities, we find that 8.00, 18.41, 16.86, 7.05, and 11.77 times fewer emissions are needed at Hartsfield-Jackson Atlanta International Airport (ATL), Denver International Airport (DEN), John F. Kennedy International Airport (JFK), Los Angeles International Airport (LAX), and Chicago O'Hare International Airport (ORD), respectively to decrease concentrations of $PM_{2.5}$ from nonattainment levels of 14 $\mu g/m^3$ to attainment levels of 12 $\mu g/m^3$.

Chapter 1

Introduction

1.1 Aviation

The aviation sector has seen substantial growth in the past decade with air carriers flying 631 million passenger miles in the year 2015, resulting in an increase of around 11 % over the past ten years [1]. This growth is expected to continue with the Federal Aviation Administration forecasting a 2.1 % increase in U.S. carrier passenger growth each year for the next 20 years, and a 2.1 % and 3.5 % growth in system traffic in revenue passenger miles over the next 20 years for domestic travel and international travel, respectively [2].

This projected growth can place a burden on atmospheric air quality as aircraft attributable emissions become a major component of all traffic related emissions. Aircraft emissions contribute to the overall air quality through emissions of nitrogen oxides (NO_X), sulfur oxides (SO_X), volatile organic compounds (VOC), primary elemental carbon (PEC), primary organic carbon (POC), and primary sulfate (PSO_4) during an aircraft's entire flight (takeoff to landing). These emissions can lead to the formation of air pollutants such as O_3 and $PM_{2.5}$. Air pollutant formation from aviation emissions can be considered a regional problem when emissions from landing and takeoff (LTO) operations affect populations near airports, and it can be considered a global problem when emissions from higher-altitude cruise operations affect the global atmospheric chemistry. Hence, in order to understand the overall impact from aviation emissions, we need to understand the role of these emissions in forming air pollutants.

1.2 Particulate Matter

The U.S. Environmental Protection Agency (EPA) has designated six criteria air pollutants to be regulated under the National Ambient Air Quality Standards (NAAQS) section of the Clean Air Act [3]. These six air pollutants are particulate matter (PM_{10}, $PM_{2.5}$), ozone (O_3), sulfur dioxide (SO_2), nitrogen dioxide (NO_2), carbon monoxide (CO), and lead (Pb). Regulations were devised for human health protection, however, these air pollutants have broader implications that impact the climate and chemistry of the atmosphere. In this study we will focus our efforts on PM and O_3 formation from aircraft emissions.

PM can affect human health [4, 5, 6, 7, 8, 9, 10, 11], Earth's climate [12], visibility [13, 14], and climate change uncertainty through indirect radiative forcing [12, 13, 14, 15, 16, 17, 18, 19, 20, 21]. Particulate matter refers to all internally and externally mixed particles found in the atmosphere. The solid or liquid mixture can vary in composition and formation, but the main measure of particulate matter is mass concentration. Particulate matter is classified by its aerodynamic diameter and current air quality standards have distinguished mixtures associated with adverse health effects having less than 10μm (PM_{10}) and less than 2.5μm ($PM_{2.5}$) aerodynamic diameters. However, the degree of health impact varies amongst PM components [22, 23]. Sources for combustion-related PM include industrial combustion, transportation related combustion (Including motor-vehicles, aircraft, and marine vessels), and biomass burning. PM can be directly emitted or it can formed in the atmosphere. These distinctions are labeled as primary PM and secondary PM, respectively. NAAQS have designated annual concentrations greater than $12\mu g/m^3$ and daily concentrations greater than $35\mu g/m^3$ to be harmful.

1.3 Ozone

Like PM, Ozone (O_3) has also been designated a standard under the NAAQS, and in 2015 it was revised to an even more stringent standard [24]. Primary and secondary concentration of O_3 higher than 0.070 parts per million (ppm) averaged over an 8-hour daily period is considered harmful. Tropospheric O_3 largely arises from a series of reactions initiated by sun light, involving nitrogen dioxide (NO_2) and volatile organic compounds (VOCs). The availability of NO_2 and VOCs in the lower atmosphere is largely influenced by anthropogenic sources. Nitrogen oxide (NO) emissions from mobile and stationary combustion processes react with O_3 and other radicals to form NO_2, and VOCs can be directly emitted from the same combustion processes.

Other anthropogenic emissions, such as SO_2, can effect tropospheric O_3 formation indirectly by affecting the tropospheric chemistry that governs the availability of O_3 precursors. Even PM has recently been linked to influencing tropospheric O_3 chemistry through radiative forcing feedback [25, 26, 27, 28, 29, 30, 31, 32, 33].

Impacts from O_3 include environmental impacts and human health impacts. O_3 can limit plant and crop growth when they are exposed to higher levels of O_3 [34], and human exposure to O_3 has been linked to impaired lung and cardiovascular functions [35, 36, 37].

With regards to our mobile source sector of interest contributing to combustion-related air pollution emissions, $PM_{2.5}$ contributions from aviation are expected to increase with LTO aircraft operations increasing annual average concentrations of $PM_{2.5}$ from 0.05% to 0.20% by 2025 [38]. An increase in aviation emissions will lead to a larger impact on health with one study on 99 U.S. airports estimating an increase in premature deaths due to aviation emissions from 75 deaths in 2005 to 460 deaths in 2025 [39]. Our study will look to understand how aviation emissions during LTO operations affect the formation of $PM_{2.5}$ and O_3.

Chapter 2

Methods

2.1 Air Quality Modeling

In this work we utilize an Eulerian atmospheric chemical transport model (CTM) to quantify the concentration and transport of PM, O_3, and other pollutants in a 36×36 km grid cell resolution domain. We assume each chemical species in each grid cell to be well mixed and the model generates a concentration of each chemical species at each time step. The Community Multiscale Air Quality modeling system (CMAQ) [40], an Eulerian atmospheric CTM, has been used in this work.

Most Eulerian atmospheric CTMs calculate chemical species concentrations in each grid cell at each time step by solving the advection-diffusion-reaction equation (Eq. 2.1).

$$\frac{dC_i}{dt} = -\nabla(\vec{u}\ C_i) + \nabla(\vec{K}\ C_i) + R_i + E_i \tag{2.1}$$

In the advection-diffusion-reaction equation, C_i is the concentration of a chemical species denoted with subscript i, $\vec{u}$ is the wind field, $\vec{K}$ is the turbulence diffusivity tensor, R_i is the reaction rate of species i, and E_i is the emission rate of chemical species i. This ordinary differential equation describes the change in concentration of any chemical species in the model over time.

2.2 Decoupled Direct Method

Various sensitivity analyses in the atmospheric CTM framework are used for guiding policy and environmental scenarios. One simple and commonly used method is the Brute Force method which relies on a subtractive or finite-difference analysis approach. For this analysis, at least two model simulations are run with one case having some input parameter varied and the other case is left unchanged. The difference between the two cases describes the effect of the varied input parameter. This can be done for as many scenarios as needed with each scenario requiring two model simulations.

The advantage of the Brute Force (BF) method is its simplicity. Most other sensitivity analyses methods are compared with the BF method. Limitations of the BF method include the computational cost required for performing multiple scenarios and the often noisy output concentrations that may arise when input parameters are varied by small amounts. We use a sensitivity analysis method that can handle multiple scenarios and reduce the noise from small variations. This method is known as the Decoupled Direct Method in Three Dimensions (DDM-3D) [41, 42, 43].

While BF methods are performed with output from model simulations, DDM-3D is performed within the model at each time step. Derivatives are taken at each time step which calculate the change in concentration of a chemical species with respect to some change in an input parameter. In the CMAQ DDM-3D framework, input parameters that can be varied include initial conditions, boundary conditions, emissions, and reaction rates. Output from DDM-3D is in the form of sensitivity coefficients which express the derivatives taken at each time step (Eq. 2.2).

$$S^1_{i,j} = \frac{\partial C_i}{\partial E_j} \tag{2.2}$$

Equation 2.2 shows the form of the sensitivity coefficient S as calculated in the DDM-3D analysis. The superscript ^{1} denotes a first order change to some chemical species C_i with respect to a varying input parameter E_j. In our case we will only concern ourselves with varying emission input parameters, as denoted by E. These sensitivity coefficients will propagate through our model simulation and CMAQ DDM-3D provides the solution to a modified advection-diffusion-reaction equation (Eq. 2.3).

$$\frac{\partial S^1_{i,j}}{\partial t} = -\nabla(\vec{u}\ S^1_{i,j}) + \nabla(\vec{K}\ S^1_{i,j}) + J_i\ S^1_j + E_i \tag{2.3}$$

The modified advection-diffusion-reaction equation is in terms of the first order sensitivity coefficients $S^1_{i,j}$ and J_i denotes the i-th row of a Jacobian matrix of reaction rates. First order sensitivity coefficients describe linear changes in concentrations with respect to changing emissions. In our case of air pollutants attributable to aviation emissions, we need to be concerned with air pollutant species that may not be linearly dependent on aviation emissions. The chemistry surrounding tropospheric $PM_{2.5}$ and O_3 formation is far more complicated than what can be expressed with only first order changes. Hence, we will extend our DDM-3D analysis framework to what is known as higher order decoupled direct method in three dimensions (HDDM-3D) in order to calculate second order sensitivity coefficients. In doing so, we hope to capture more of the chemistry related to $PM_{2.5}$ and O_3 formation from aviation emissions to understand how aviation impacts air pollution.

2.3 Higher Order Decoupled Direct Method

Here we will outline two types of second order sensitivity coefficients. Full derivations of HDDM-3D can be found in Hakami et. al 2003 [44] and Zhang et. al 2012 [45] with the latter paying special attention to the treatment of Secondary Organic Aerosols (SOA) within the HDDM-3D framework.

One type of second order sensitivity coefficient is calculated by simply taking the second derivative of Eq. 2.2 with respect to parameter E_j.

$$S^2_{i,j} = \frac{\partial^2 C_i}{\partial E_j^2} \tag{2.4}$$

Eq. 2.4 is the second order change of a species C_i with respect to some varying input paramter E_j. The second type of second order sensitivity coefficient relies on the separability of the partial differential equations that govern atmospheric CTMs. HDDM-3D can also calculate second order cross-sensitivity coefficients that describe the change in concentration of chemical species C_i with respect to *two* varying input parameters E_j and E_k (Eq. 2.5).

$$S^2_{i,j,k} = \frac{\partial^2 C_i}{\partial E_j \partial E_k} \tag{2.5}$$

The resulting advection-diffusion-reaction equation with second order cross-sensitivity coefficients can be written in a simplified form as:

$$\begin{aligned}\frac{\partial S^2_{i,j,k}}{\partial t} = &-\nabla(\vec{u}\ S^2_{i,j,k}) + \nabla(\vec{K}\ \nabla S^2_{i,j,k}) + \\ &\vec{J_i}\ \vec{S}^2_{j,k} + f(C_i, S^1_{i,j}, S^1_{i,k}, \vec{u}, \vec{K}, R_i, E_i).\end{aligned} \tag{2.6}$$

In Eq. 2.6, superscripts ^{1} and ^{2} denote first order and second order sensitivity coefficients, respectively. $\vec{J_i}$ is i-th row of a Jacobian matrix of reaction rates and $\vec{S}^2_{j,k}$ is a vector of second order sensitivity coefficients. For brevity, the function f contains the relationships between the concentration of species i, first order sensitivity coefficients with respect to parameters j and k, the wind and turbulence diffusivity tensors, and the reaction and emission rates of species i. In this general form, the equation can be applied to any varying

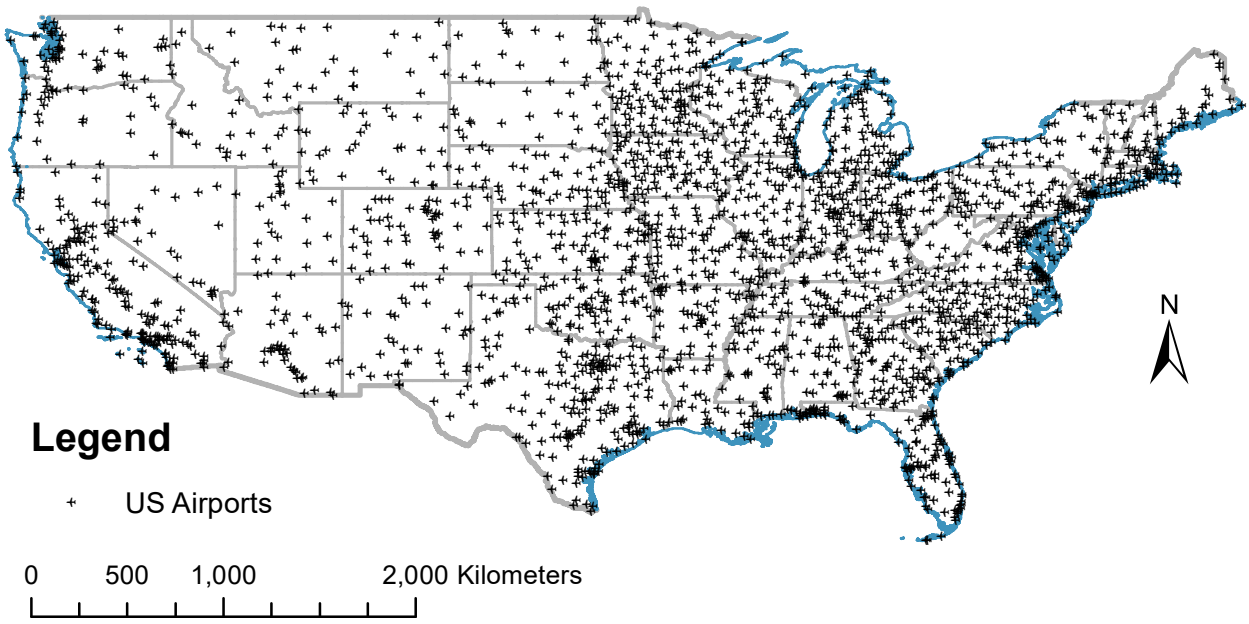

Figure 2.1: Locations of the 2,106 active airports considered in our CONUS domain.

input parameter, not just changes to emissions. Details of this function f can be found in Eq. (9) in Hakami et al. 2003 [44].

For our study, six precursor emissions that are responsible for the formation of $PM_{2.5}$ and O_3 are chosen as sensitivity parameters for first order DDM-3D analyses. Three gas phase species; nitrogen oxides (NO_X), sulfur dioxide (SO_2), volatile organic compounds (VOC), and three particle phase species; primary elemental carbon (PEC), primary organic carbon (POC), and primary sulfate (PSO_4) are directly emitted from aircrafts and they all can lead to the formation of $PM_{2.5}$ and O_3 in the atmosphere. We limit our sensitivity parameters for second order HDDM-3D analyses to the three gas phases species since these species are responsible for secondary formation of pollutants in the atmosphere. Table 2.1 shows the species included in the CMAQ simulation for our precursor emissions.

2.4 Domain

Our domain consists of the continental United States (CONUS) with a 148 × 112 grid of 36km × 36km resolution. We utilize the FAA's Aviation Emission Design Tool (AEDT) [46] for constructing aircraft flight segments from the 2,106 active airports in the United States. Figure 2.1 shows all of the airports considered in our domain. We consider only landing and takeoff flight segments; that is all flight segments below 3,000 ft. By considering only LTO operations, we are focusing our efforts on effects from aircraft emissions at a regional level. And although our model simulation is performed with 34 vertical layers into the atmosphere, we will consider DDM-generated sensitivities within the model at only the surface layer for the purpose of understanding health impacts in populations located near airports.

LTO segments are processed into gridded emission rate files using AEDTProc [47]. Background emission rates, defined to be all non-aviation related emissions, from EPA's National Emissions Inventories (NEI-2005) [48] are processed into gridded emission rate files using the Sparse Matrix Operator Kernal Emissions (SMOKE) [49]. Meteorology data for 2005 is from the Weather Research and Forecasting model (WRF) [50], with outputs downscaled from NASA's Modern-Era Retrospective Analysis for Research and Applications data (MERRA) [51]. 2005 Boundary conditions are derived from global CAM-chem simulations [52]. Simulations are performed for the months of January and July in 2005 with a 10 day spin up for each month. January and July are chosen to approximately represent winter and summer characteristics seen during each half of the year. Future work will expand the temporal domain over the entire year.

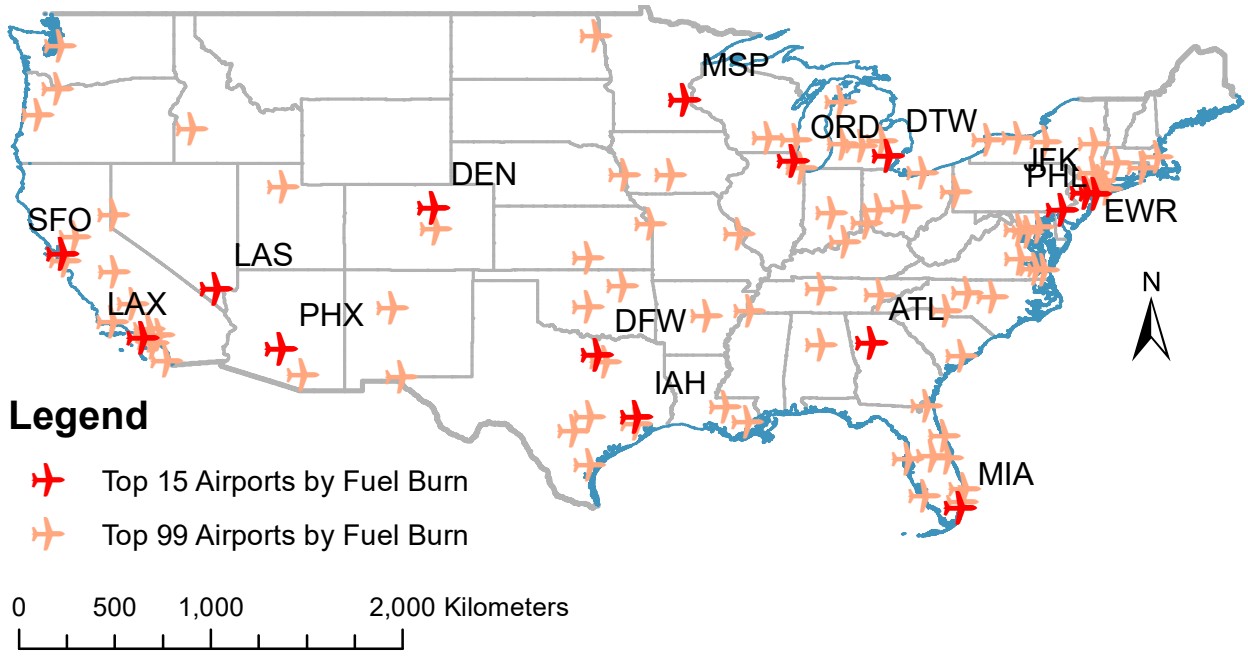

Figure 2.2: Locations of the top 99 US airports responsible for the largest total fuel burn considered in our CONUS domain. This is for purely illustrative purposes.

Group	Model Species	Name
NO_X	NO	Nitric oxide
	NO_2	Nitrogen dioxide
	HONO	Nitrous acid
EC	PEC	Primary elemental carbon
OC	POC	Primary organic carbon
SO_4	PSO4	Primary sulfate
SO_2	SO2	Sulfur dioxide
VOC	ALD2	Acetaldehyde
	ALDX	Ethene
	ETHA	Ethane
	ETOH	Ethanol
	FORM	Formaldehyde
	IOLE	Internal olefin bond
	MEOH	Methanol
	OLE	Terminal olefin bond
	TOL	Toluene-like
	XYL	Xylene-like

Table 2.1: Sensitivity parameters as defined in the model

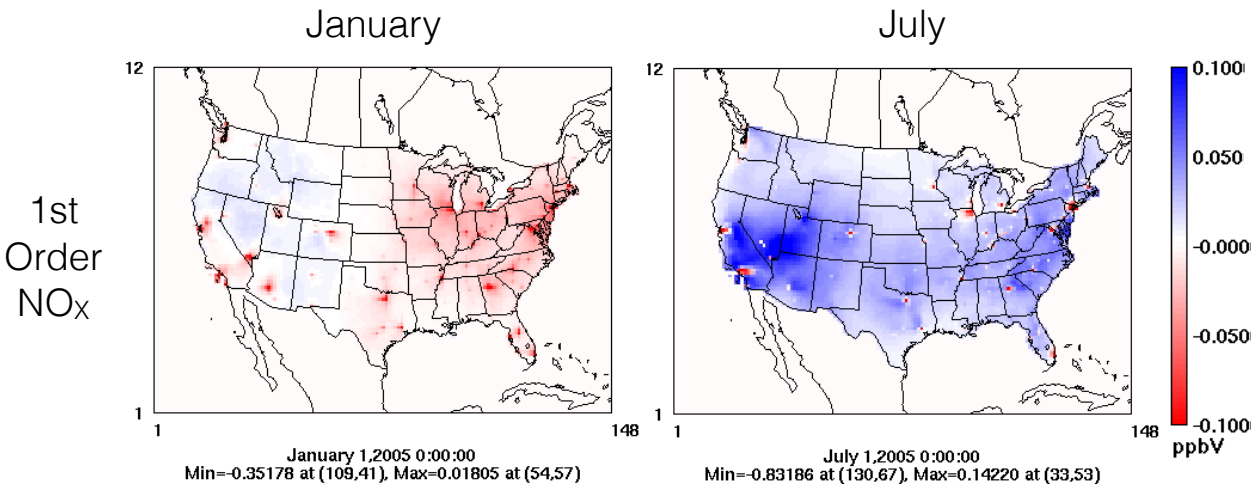

Figure 3.1: First order sensitivity calculations of O_3 concentration (in ppbV) with respect to NO_X emissions for the months of January and July.

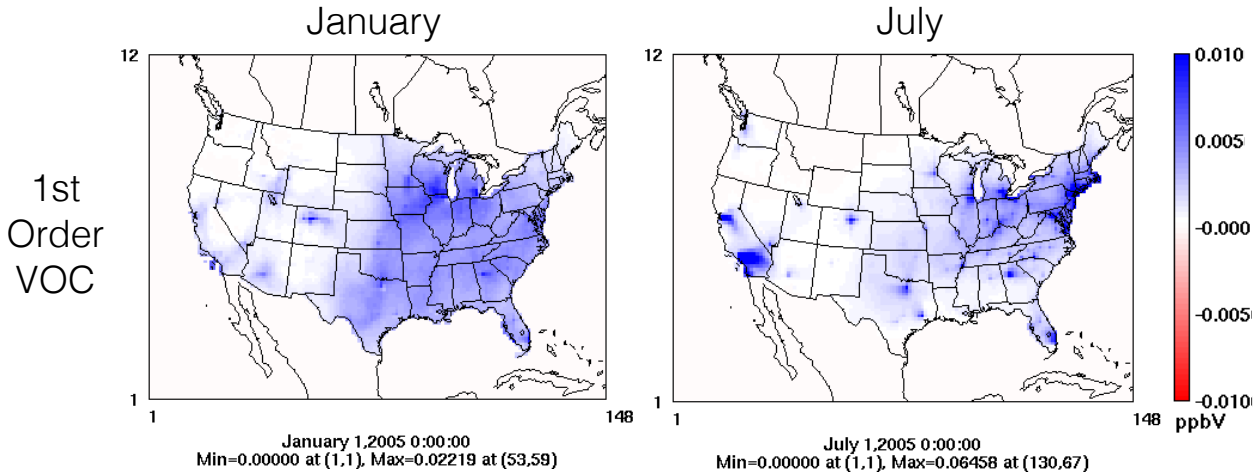

Figure 3.2: First order sensitivity calculations of O_3 concentration (in ppbV) with respect to VOC emissions for the months of January and July.

Chapter 3

Results

3.1 O_3 First Order Response

We begin with calculating first order sensitivity coefficients as a way to estimate where nonlinearity, or second order changes in concentration, is important in our domain. Beginning with O_3 concentration sensitivities to our aircraft percursor emissions, we can look at O_3 first order sensitivities to NO_X (90% NO, 9% NO_2, and 1% HONO for aviation emissions) and VOC aviation emissions.

Figures 3.1 and 3.2 show the DDM first order sensitivity coefficients for O_3 sensitivity to NO_X and VOC emissions, respectively. Seasonal differences indicate a nonlinear concentration response to NO_X emissions with an indication of a possible chemical regime change in July. Chemical regime refers to whether an area is considered to be NO_X-limited or NO_X-inhibited (VOC limited). Tropospheric O_3 formation is predicated by the availability of NO_X and VOCs in a given region reacting with the OH radical [53]. And since NO_X and VOCs compete for available OH in the atmosphere, the O_3 formation pathways can vary based on the

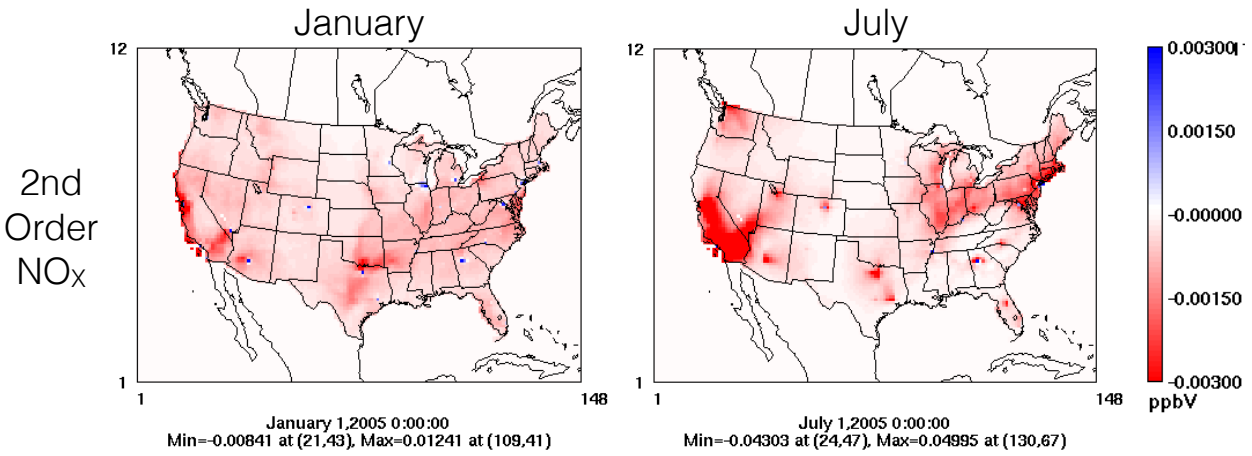

Figure 3.3: Second order sensitivity calculations of O_3 concentration (in ppbV) with respect to NO_X emissions for the months of January and July.

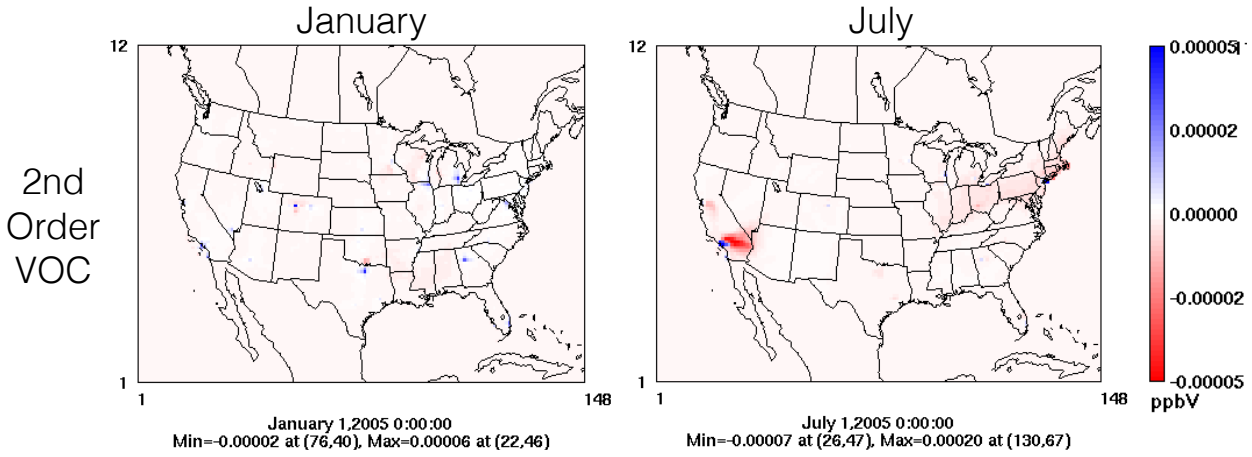

Figure 3.4: Second order sensitivity calculations of O_3 concentration (in ppbV) with respect to NO_X emissions for the months of January and July.

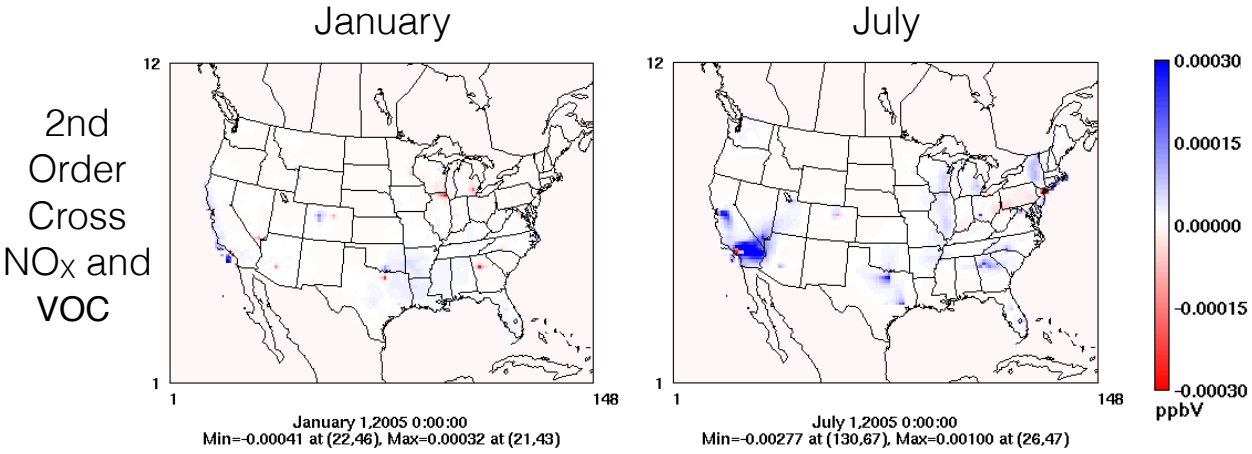

Figure 3.5: Second order sensitivity calculations of O_3 concentration (in ppbV) with respect to NO_X and VOC emissions for the months of January and July.

emissions of VOCs or NO_X in a region. Regions with high NO_X emissions leading to O_3 formation are deemed NO_X-inhibited (VOC-limited) and are often highly localized to urban regions. Regions where available VOCs are comparable to available NO_X are deemed NO_X-limited and tend to categorize most suburban to rural areas. However, it is not the case that simply reducing emissions of NO_X in a NO_X-inhibited regime or reducing VOCs in a NO_X-limited regime will lead to reductions of O_3. Due to the nonlinearity of O_3 production pathways, emission control strategies for reducing O_3 differ based on which chemical regime one may be in. EKMA diagrams were one of the first analyses to show how O_3 concentrations change with reductions of NO_X and VOCs in NO_X-inhibited and NO_X-limited regimes [54]. They rely on knowing the O_3 concentrations for varying amounts of NO_X and VOCs in a given region. This makes them hard to replicate from a modeling perspective since each varied amount of NO_X and VOCs require an additional modeling simulation. DDM and HDDM is advantageous in this respect [55, 56, 44] since their outputs allow for a comprehensive understanding of how O_3 concentrations change with respect to varying NO_X and VOC emissions across our domain. Chemical regimes will be indicated by how O_3 either increases or decreases with respect to increasing or decreasing NO_X and VOC emissions.

Negative first order sensitivity coefficients with respect to NO_X emissions in the immediate proximity of the major U.S. airports indicate a NO_X-inhibited regime for January and July. However, regions of positive first order sensitivity coefficients (Downwind of SFO, LAX, ATL) in the month of July indicate a shift to a NO_X-limited regime. First order sensitivity to VOC emissions exhibits a largely linear behavior with positive first order sensitivity coefficients across the entire domain. Hence, using first order DDM analyses, we can estimate where nonlinear changes in O_3 become important. In our case, this nonlinearity represents a chemical regime change downwind of larger urban airports.

3.2 O_3 Second Order Response

Figures 3.3 and 3.4 show the HDDM second order sensitivity coefficients for O_3 sensitivity to NO_X and VOC, respectively. As we had anticipated from the first order responses to VOC emissions, O_3 concentration response is mostly linear and second order sensitivity coefficients are one to two orders in magnitude smaller than first order sensitivity coefficients. Nonlinearity can be seen in the immediate vicinity of Los Angeles and downwind of LAX in the month of July.

Lastly, we can examine the second order cross-sensitivity of O_3 concentration response to both NO_X and VOC emissions. Figure 3.5 shows the HDDM second order cross-sensitivity coefficients for O_3 sensitivity to NO_X and VOC emissions in our domain. Cross-sensitivity responses are inherently more complicated to conceptualize, with the concentration response now determined by variations of two types of emissions. This becomes important for describing the formation of O_3 in terms of which chemical regime, NO_X-limited or NO_X-inhibited, one may be concerned with. In a NO_X-limited regime, O_3 production (denoted as P_{O_3}) is linearly dependent on NO (Eq. 3.1).

$$P_{O_3} \sim NO \tag{3.1}$$

In a NO_X-inhibited regime, O_3 formation is linearly dependent on VOCs and inversely dependent on NO_2.

$$P_{O_3} \sim \frac{VOC}{NO_2} \tag{3.2}$$

In our case, we can clearly distinguish NO_X-limited and NO_X-inhibited regimes by looking at cross-sensitivity coefficients. If we consider LAX and the region downwind, our second order cross-sensitivity coefficients are negative in the immediate area surrounding LAX and positive downwind. And since we know our first order sensitivity coefficients to NO_X to be one to two orders of magnitude higher than our sensitivity coefficients to VOC, the region immediately surrounding LAX is NO_X-inhibited while the rural downwind area is NO_X-limited. The transition between regimes can be seen with our nonzero second order sensitivity coefficients. NO_X availability governs O_3 formation and NO_X emissions from aircrafts are responsible for the highest degree of nonlinear behavior when considering O_3 precursor emissions from aircrafts.

3.3 $PM_{2.5}$ First Order Response

Figure 3.6 and 3.7 show $PM_{2.5}$ first order sensitivity coefficients with respect to our six varying precursor emissions: NO_X, SO_2, VOC, PEC, POC, and PSO_4. Although we have emissions from 2,106 airports in our domain, significant impacts (values on the order of 10^{-3}) are seen at only major airports (Fig. 2.2). This can be seen by looking at $PM_{2.5}$ sensitivities to our particle phase species, PEC, POC, or PSO_4 where the impact on PM formation from these precursors are highly localized to the points of emission; in this case, the major airports (Fig. 3.7). This PM formation can be considered primary while $PM_{2.5}$ sensitivities to NO_X, SO_2, and VOC are significant up to several hundred kilometers from the emission source indicative of secondary PM formation.

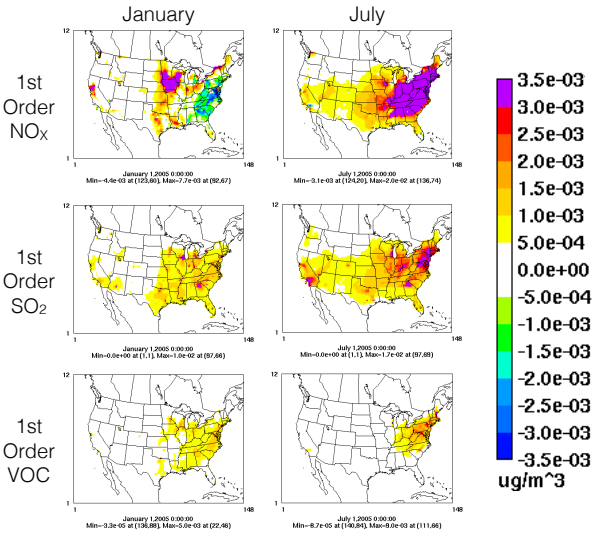

Figure 3.6: First order sensitivity calculations of $PM_{2.5}$ concentration (in $\mu g/m^3$) with respect to NO_X, SO_2, and VOC emissions for the months of January and July.

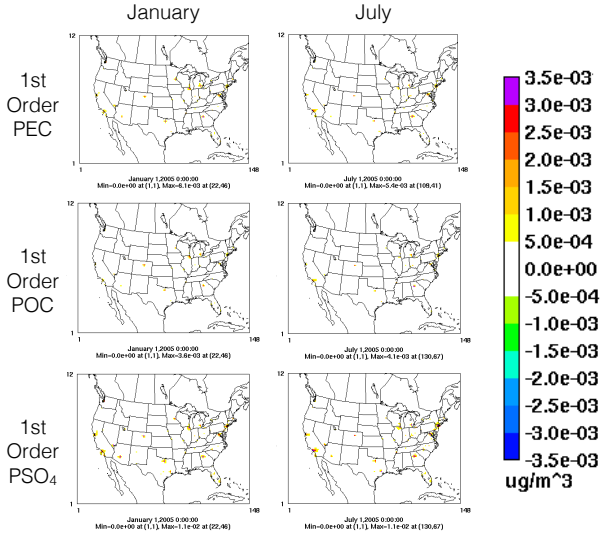

Figure 3.7: First order sensitivity calculations of $PM_{2.5}$ concentration (in $\mu g/m^3$) with respect to PEC, POC, and PSO_4 emissions for the months of January and July.

Seasonal differences indicate larger first order sensitivity coefficients across all precursor emissions in the month of July than January. The only significant negative first order sensitivities are seen with respect to NO_X emissions. In January, large areas of negative first order sensitivity coefficients are seen in the southeast U.S. stretching up the coast. In July, this same region becomes positive and the few areas that exhibit negative first order coefficients are Los Angeles and downwind of LAX, the Miami area, Chicago, and San Francisco.

3.4 $PM_{2.5}$ Second Order Response

Figure 3.8 shows the second order sensitivity coefficients for $PM_{2.5}$ with respect to NO_X, SO_2, and VOC emissions. We can see the most second order impact of $PM_{2.5}$ with respect to NO_X emissions. And although aircrafts are not direct emitters of ammonia (NH_3), availability of NH_3 can affect the partitioning of secondarily formed nitrate into particle phase owing to the overall $PM_{2.5}$ formation [57]. One work has studied how the availability of NH_3 impacts aviation-attributable emissions [38]. NH_3 availability affecting the partitioning of secondarily formed nitrate into particle phase is evident by looking at NO_X nonlinear sensitivities in regions where background NH_3 is available to affect nitrate formation, such as the southeast U.S. and the midwest U.S. during winter months.

Similar to NH_3 availability affecting secondary nitrate formation, oxidant availability can affect secondary sulfate and nitrate formation. This arises through indirect effects often attributable to sensitivities to two or more precursors. HDDM becomes a perfect method for capturing these indirect effects by calculating sensitivities to multiple inputs. Figure 3.9 shows the second order cross-sensitivity coefficients for $PM_{2.5}$ with respect to NO_X and SO_2 and NO_X and VOC emissions. Availability of oxidants such as HO_X radicals

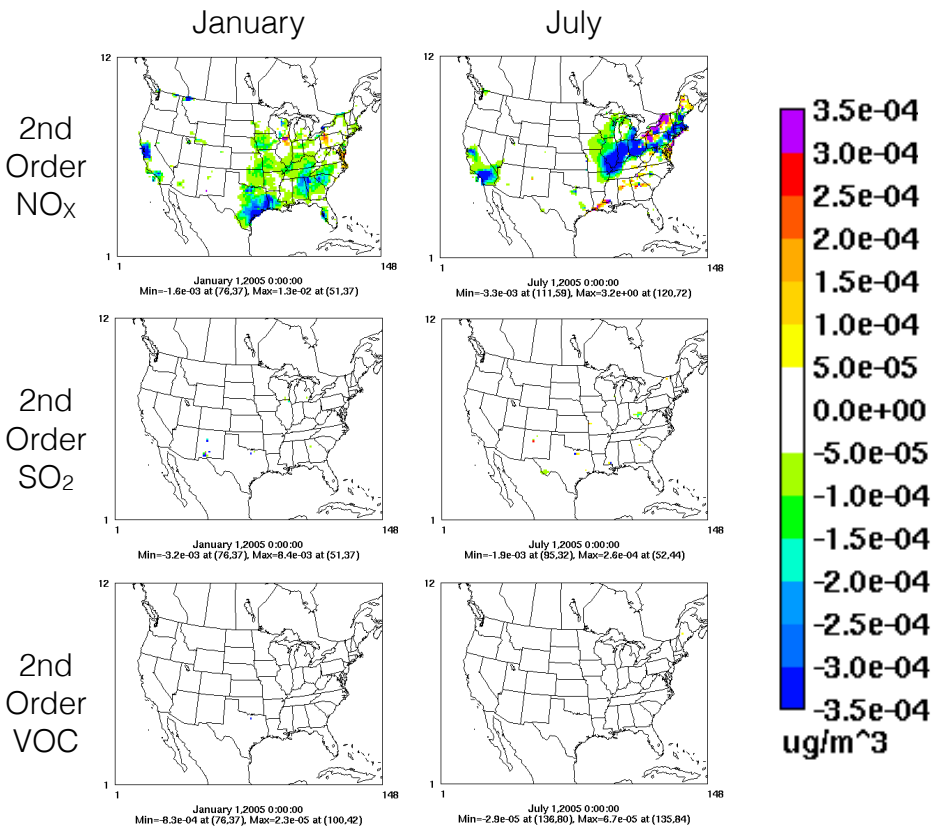

Figure 3.8: Second order sensitivity calculations of $PM_{2.5}$ concentration (in $\mu g/m^3$) with respect to NO_X, SO_2, and VOC emissions for the month of January and July.

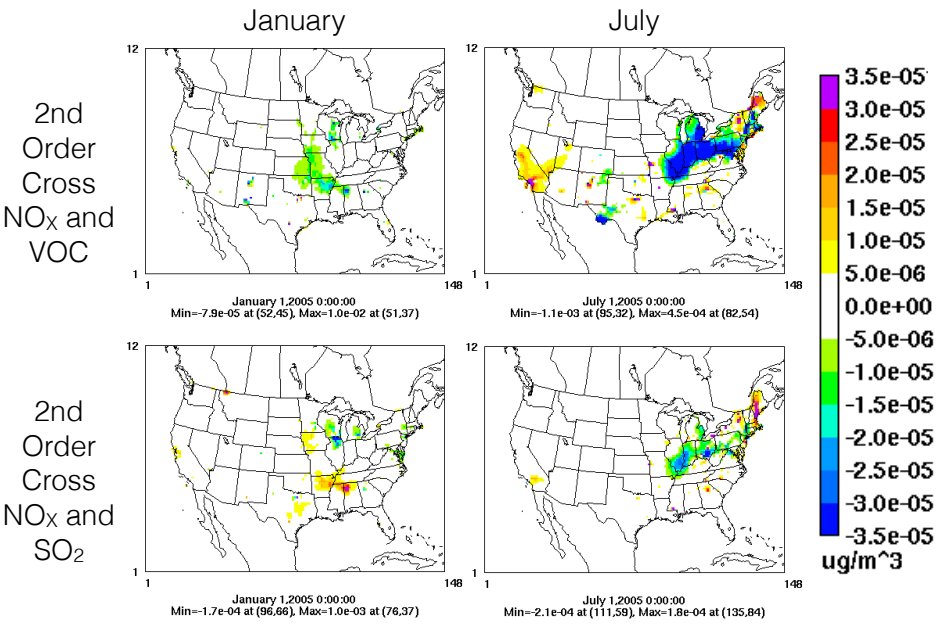

Figure 3.9: Second order cross-sensitivity calculations of $PM_{2.5}$ concentration (in $\mu g/m^3$) with respect to NO_X and SO_2 emissions, and NO_X and VOC emissions for the month of January and July.

(HO_X = OH+peroxy) and O_3 leading to oxidation of SO_2 can limit sulfate formation and add to the overall $PM_{2.5}$. If SO_2 emissions are reduced in this oxidant limiting case, more oxidants are available to convert SO_2 from other sources [57]. The oxidant limiting case is important for aircraft emissions because we are concerned with changes in SO_2 emissions that are small when compared to other SO_2 sources seen on the east coast. Oxidant limiting effects are also temperature dependent and we can see this with our second order cross-sensitivity coefficients for NO_X and SO_2 emissions for January and July. With lower temperatures in January, more nitric acid (HNO_3) can dissolve into water which means NO_X aircraft emission reductions also reduces the aqueous phase acidity. This then increases sulfate formation as more SO_2 dissolves and then oxidizes in the aqueous phase [57]. With higher temperatures in July, oxidant availability is limited by reducing NO_X emissions, leading to less oxidation of SO_2 and sulfate formation beyond sulfate reduction through SO_2 emissions reduction alone. We can see these seasonal differences in figure 3.9 with July showing a large area of negative cross sensitivities to NO_X and SO_2 emissions in the Ohio valley stretching over to the east coast and an area of positive cross sensitivities to NO_X and SO_2 emissions downwind of LAX where SO_2 background emissions are considerably less.

Although the effects are smaller, oxidant availability altered by reductions in NO_X emissions can also effect secondary organic aerosols formed through oxidation of VOC emissions. We can see this nonlinear behavior in figure 3.9 for $PM_{2.5}$ cross sensitivities to NO_X and VOC aircraft emissions. Therefore, NO_X emissions are responsible for the largest amount of nonlinear behavior.

Chapter 4

Attainment Analyses

4.1 Emission Reductions

The true power of these sensitivity coefficients and the decoupled direct method in general, is its ability to estimate changes in pollutant concentrations with respect to emission reductions by only performing one model simulation. This allows for a quick and accurate way to understand how emission reductions will impact air pollutant concentrations. First and second order sensitivity coefficients can be used in simple Taylor series approximations to estimate some change in pollutant concentration, C_i, with respect to some change in emissions, $\Delta\epsilon_j$ (Eq. 4.1) [44].

$$C_i(\Delta\epsilon_j) = C_i(0) + \Delta\epsilon_j S^1_{i,j}(0) + \frac{\Delta\epsilon_j^2}{2} S^2_{i,j}(0) \tag{4.1}$$

130 airports in the United States are currently located in areas designated as being in nonattainment of the EPA's NAAQ standards [59]. Figure 4.1 shows the locations of these 130 airports (4 located in Alaska are not shown). The airports located in regions of nonattainment of these standards pose a risk to public health by contributing to the amount of air pollutants in the region. And as aviation continues to grow as an emission sector, aviation-related health impacts will affect areas already in nonattainment. We can use DDM-3D analyses to look at the effects from individual airports. First order sensitivity coefficients were calculated for emissions from five individual airports: Chicago O'Hare International Airport (ORD), Hartsfield-Jackson Atlanta International Airport (ATL), Denver International Airport (DEN), Los Angeles International Airport (LAX), and John F. Kennedy International Airport (JFK). Table 4.1 shows the first order sensitivity coefficients for each precursor emission species. Second order sensitivity coefficients were calculated as well with table 4.2 showing second order sensitivity coefficients for all gas phase species of interest, and table 4.3 showing second order sensitivity order cross-sensitivity coefficients to NO_X and SO_2 emissions and NO_X and VOC emissions. These coefficients are values calculated at each of the airport's home grid cell, referring to impacts that would be seen within that grid cell. Hence, these coefficients can vary for regions surrounding the airport's grid cell and need to be considered when considering large populations that may be downwind of airports where the coefficient may represent secondary chemistry and meteorological impacts.

We can perform a Taylor series expansion with these sensitivity coefficients to estimate the amount of emission reductions needed to bring a region that is in nonattainment of $PM_{2.5}$ standards into attainment. If we imagine the region immediately surrounding Chicago O'Hare airport (ORD's home grid cell) to be in nonattainment with a concentration of $PM_{2.5}$ of 14 $\mu g/m^3$, we can estimate the amount of emission

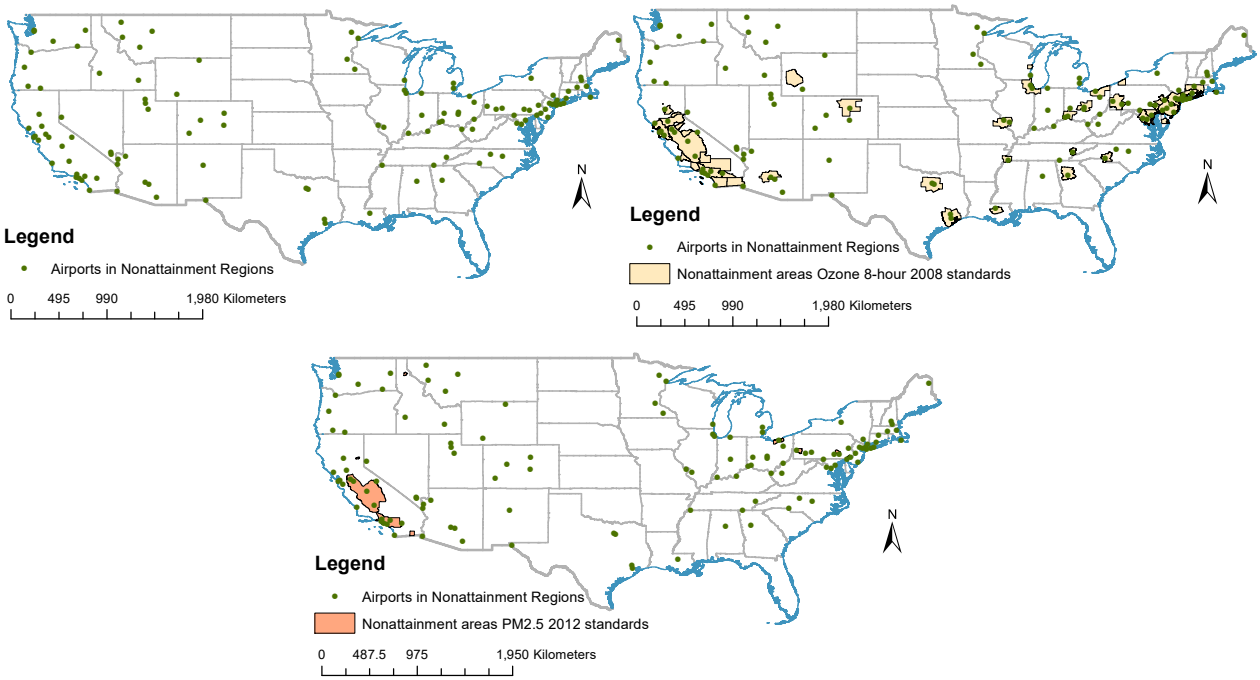

Figure 4.1: Locations of the 130 airports in regions designated as being in nonattainment by the EPA [58]

reductions needed for a decrease of $2\mu g/m^3$. Sensitivities in January are assumed to be the same for six months of the year and sensitivities in July are assumed to be the same for the other six months of the year. Using only first order sensitivity coefficients to our precursor emissions and Eq. 4.1, we would need to decrease emissions by 11.77 times in the Chicago O'Hare airport grid cell to decrease the concentration of $PM_{2.5}$ by 2 $\mu g/m^3$. We expect larger effects to be seen by including second order sensitivity coefficients for O_3 reductions and $PM_{2.5}$ reductions in airports like Los Angeles International where second order coefficients are all negative for gas phase species. Table 4.4 shows the emission reductions needed to decrease $PM_{2.5}$ by 2 $\mu g/m^3$ for each of our five airports.

Equations 4.2 through 4.4 show how the emission amounts were calculated for our individual airports' sensitivity coefficients. We show the first order calculations with respect to our precursor emissions. Equation 4.2 shows the amount of emission reduction needed, $\Delta\epsilon$, to bring a region into attainment where $C_{PM_{2.5}}(\Delta\epsilon) = 2\ \mu g/m^3$ when we only consider first order sensitivities to our precursor emissions, $S^{\mathbf{1}}_{PM_{2.5}}$. Equation 4.4 shows the approximate yearly first or second (denoted with boldface superscripts $^{\mathbf{1,2}}$, while normal expressions raised to a power are not boldfaced) sensitivity coefficients with values from tables 4.1 and 4.2. Future work will utilize equation 4.3. This is the same calculation but it now includes the second order term in the Taylor series expansion which takes into account second order sensitivities.

$$C_{PM_{2.5}}(\Delta\epsilon) = \Delta\epsilon S^{\mathbf{1}}_{PM_{2.5}} \tag{4.2}$$

$$C_{PM_{2.5}}(\Delta\epsilon) = \Delta\epsilon S^{\mathbf{1}}_{PM_{2.5}} + \frac{\Delta\epsilon^2}{2} S^{\mathbf{2}}_{PM_{2.5}} \tag{4.3}$$

$$\begin{aligned} S^{\mathbf{1,2}}_{PM_{2.5}} = 6\big[&S^{\mathbf{1,2}}_{PM_{2.5},NO_x} + S^{\mathbf{1,2}}_{PM_{2.5},SO_2} + S^{\mathbf{1,2}}_{PM_{2.5},VOC} + S^{\mathbf{1,2}}_{PM_{2.5},POC} + S^{\mathbf{1,2}}_{PM_{2.5},PEC} + S^{\mathbf{1,2}}_{PM_{2.5},PSO_4}\big]_{JAN} \\ +6\big[&S^{\mathbf{1,2}}_{PM_{2.5},NO_x} + S^{\mathbf{1,2}}_{PM_{2.5},SO_2} + S^{\mathbf{1,2}}_{PM_{2.5},VOC} + S^{\mathbf{1,2}}_{PM_{2.5},POC} + S^{\mathbf{1,2}}_{PM_{2.5},PEC} + S^{\mathbf{1,2}}_{PM_{2.5},PSO_4}\big]_{JUL} \end{aligned} \tag{4.4}$$

	ORD		ATL		DEN		LAX		JFK	
	January	July	January	July	January	July	January	July	January	July
O_3 to NO_x	−0.219	−0.315	−0.344	−0.361	−0.238	−0.227	−0.192	−0.617	−0.214	−0.827*
O_3 to VOC	0.006	0.010	0.005	0.018	0.003	0.014	0.006	0.019	0.001*	0.055
$PM_{2.5}$ to NO_x	4.626×10^{-5}*	−0.003	−0.003	−0.002*	−0.001	−0.002	0.002	−0.003	−0.001	−0.014
$PM_{2.5}$ to SO_2	0.010	0.002	0.009	0.007	3.940×10^{-4}*	0.002	0.002	0.003*	0.002	0.006
$PM_{2.5}$ to VOC	0.002	2.773×10^{-4}	0.001*	4.580×10^{-4}	0.001	2.118×10^{-4}	0.005	0.002	0.001	0.003
$PM_{2.5}$ to PEC	0.004	0.002	0.004	0.005	0.003	0.002	0.006	0.005	0.001	0.004
$PM_{2.5}$ to POC	0.002	0.001	0.002	0.003	0.003	0.002	0.003	0.003	0.001	0.004
$PM_{2.5}$ to PSO_4	0.005	0.003	0.005	0.008	0.004	0.003	0.011	0.009	0.002	0.010

Table 4.1: First order sensitivity coefficients of O_3 (ppb) and $PM_{2.5}$ ($\mu g/m^3$) at each airport's home cell. * Respective maximum or minimum not located in airport home grid cell

	ORD		ATL		DEN		LAX		JFK	
	January	July	January	July	January	July	January	July	January	July
O_3 to NO_x	0.008	0.002	0.013	0.014	0.009	0.001	0.006	0.017	0.004	0.047
O_3 to VOC	2.341×10^{-5}	4.949×10^{-6}	3.279×10^{-5}	9.873×10^{-6}	1.005×10^{-5}	8.885×10^{-6}	5.414×10^{-5}	1.567×10^{-4}	5.079×10^{-6}	1.677×10^{-4}
$PM_{2.5}$ to NO_x	1.287×10^{-4}	5.609×10^{-5}	2.417×10^{-5}	1.037×10^{-4}	1.009×10^{-5}	-1.857×10^{-5}	-1.071×10^{-4}	-2.018×10^{-4}	2.134×10^{-4}	1.169×10^{-3}
$PM_{2.5}$ to SO_2	-1.623×10^{-4}	-8.514×10^{-7}	$-7.167 \times^1 0{-}5$	-2.714×10^{-5}	-1.133×10^{-7}	-4.943×10^{-8}	-2.502×10^{-7}	-7.939×10^{-7}	-2.027×10^{-5}	-2.995×10^{-5}
$PM_{2.5}$ to VOC	-2.475×10^{-5}	-1.460×10^{-7}	-3.239×10^{-6}	-8.227×10^{-7}	-1.677×10^{-6}	-2.789×10^{-7}	4.654×10^{-6}	1.573×10^{-6}	-1.751×10^{-6}	-2.479×10^{-6}

Table 4.2: Second order sensitivity coefficients of O_3 (ppb) and $PM_{2.5}$ ($\mu g/m^3$) at each airport's home cell.

	ORD		ATL		DEN		LAX		JFK	
	January	July	January	July	January	July	January	July	January	July
O_3 to NO_x and VOC	-2.179×10^{-4}	-1.619×10^{-5}	-2.329×10^{-4}	3.010×10^{-5}	-8.713×10^{-5}	-8.476×10^{-5}	-3.658×10^{-4}	-0.001	-4.325×10^{-5}	-0.002
$PM_{2.5}$ to NO_x and SO_2	-9.282×10^{-6}	-2.378×10^{-5}	-3.461×10^{-5}	-2.581×10^{-5}	-4.518×10^{-6}	-1.631×10^{-5}	-1.531×10^{-5}	-5.495×10^{-5}	-9.706×10^{-6}	-1.087×10^{-4}
$PM_{2.5}$ to NO_x and VOC	-3.040×10^{-5}	7.438×10^{-7}	-2.084×10^{-5}	-1.051×10^{-6}	-1.169×10^{-5}	1.113×10^{-6}	-4.583×10^{-5}	-3.087×10^{-5}	-2.435×10^{-5}	-1.193×10^{-4}

Table 4.3: Second order cross-sensitivity coefficients of O_3 (ppb) and $PM_{2.5}$ ($\mu g/m^3$) at each airport's home cell.

$\Delta\epsilon$	ORD	ATL	DEN	LAX	JFK
First order All precursors	11.77	8.00	18.41	7.05	16.86

Table 4.4: Emission reductions needed to reduce $PM_{2.5}$ concentrations by 2 $\mu g/m^3$ at each airport's home grid cell.

Chapter 5

Conclusion

5.1 Conclusions and Future Work

We have utilized HDDM-3D as implemented in CMAQ to quantify the impacts of both NAS-wide aviation emissions and airport-specific aviation emissions on the formation of $PM_{2.5}$ and O_3. In this way, we can develop a deeper understanding of how varying aviation emissions may impact regional air quality and public health. The application of sensitivity coefficients to individual airports and precursor species allows for a more tailored approach in assessing health impacts as the aviation sector continues to grow. We found that 8.00, 18.41, 16.86, 7.05, and 11.77 times fewer emissions are needed at Hartsfield-Jackson Atlanta International Airport (ATL), Denver International Airport (DEN), John F. Kennedy International Airport (JFK), Los Angeles International Airport (LAX), and Chicago O'Hare International Airport (ORD), respectively to decrease concentrations of $PM_{2.5}$ from nonattainment levels of 14 $\mu g/m^3$ to attainment levels of 12 $\mu g/m^3$ when considering all aviation precursors to $PM_{2.5}$. A 2 $\mu g/m^3$ decrease in $PM_{2.5}$ is a large target to achieve when considering aviation emissions. This is why calculated emission reductions are large in our analysis. Since aircraft emissions are usually less than 1-5% of county-wide NO_X emissions, the general ranges of emissions reductions will be commensurate. We plan to expand this analysis for more airports in regions of nonattainment, as well as airports that are in regions of attainment to quantify the effects of aviation in relatively clean areas of the country. This will be done with 2011 emission data. We also plan to extrapolate our individual airport emission sensitivity results to sensitivities from aviation fuel burn. This can be used to help policy makers easily relate to aircraft operations at a given airport while designing effective policies.

5.2 Acknowledgements

This work was funded by ASCENT under grants to UNC. ASCENT is funded by the FAA, NASA, the U.S. Department of Defense, Transport Canada, and the EPA. The aviation emissions inventories used for this work were provided by the U.S. DOT Volpe Center and are based on data provided by the U.S. FAA and EUROCONTROL in support of the objectives of the ICAO Committee on Aviation Environmental Projection CO2 Task Group. Any opinions, finding, and conclusions or recommendations expressed in this material are those of the author(s) and do not necessarily reflect the views of the sponsors.

Bibliography

[1] U.S. Department of Transportation, *Bureau of Transportation Statistics. T-100 segment data* (2016), available at https://www.transtats.bts.gov/Fields.asp?Table_ID=293.

[2] U.S. Federal Aviation Administration, *FAA Aerospace Forecast 2016-2036* (2016), available at https://www.faa.gov/data_research/aviation/aerospace_forecasts/media/FY2016-36_FAA_Aerospace_Forecast.pdf.

[3] U.S. Environmental Protection Agency, *National Ambient Air Quality Standards (NAAQS)* (2012), available at https://www.epa.gov/criteria-air-pollutants/naaqs-table.

[4] C. A. Pope and D. W. Dockery, *Health Effects of Fine Particulate Air Pollution: Lines that Connect*, J. Air Waste Manag. Assoc. **56**, 709 (2006).

[5] J. C. Chow, J. G. Watson, J. L. Mauderly, and D. L. Costa, *Health Effects of Fine Particulate Air Pollution: Lines that Connect*, J. Air Waste Manag. Assoc. **56**, 1368 (2006).

[6] J. L. Mauderly and J. C. Chow, *Health Effects of Organic Aerosols*, Inhal. Toxicol. **20**, 257 (2008), doi: 10.1080/08958370701866008.

[7] R. Beelen, O. Raaschou-Nielsen, M. Stafoggia, Z. J. Andersen, G. Weinmayr, B. Hoffmann, K. Wolf, E. Samoli, P. Fischer, M. Nieuwenhuijsen, et al., *Effects of long-term exposure to air pollution on natural-cause mortality: An analysis of 22 European cohorts within the multicentre ESCAPE project*, The Lancet **383**, 785 (2014), doi: 10.1016/S0140-6736(13)62158-3.

[8] N. A. Clark, P. A. Demers, C. J. Karr, M. Koehoorn, C. Lencar, L. Tamburic, and M. Brauer, *Effect of early life exposure to air pollution on development of childhood asthma*, Environ. Health Persp. **118**, 284 (2010), doi: 10.1289/ehp.0900916.

[9] B. D. Ostro, W.-Y. Feng, R. Broadwin, B. J. Malig, R. S. Green, and M. J. Lipsett, *The impact of components of fine particulate matter on cardiovascular mortality in susceptible subpopulations.*, J. Occup. Env. Med. **65**, 750 (2008), doi: 10.1136/oem.2007.036673.

[10] T. Lanki, J. J. de Hartog, J. Heinrich, G. Hoek, N. A. H. Janssen, A. Peters, M. Stölzel, K. L. Timonen, M. Vallius, E. Vanninen, et al., *Can we identify sources of fine particles respnsible for exercise-induced ischemia on days with elevated air pollution? The ULTRA study*, Environ. Health Persp. **114**, 655 (2006), doi: 10.1289/ehp.8578.

[11] J. Wu, D. Houston, F. Lurmann, P. Ong, and A. Winer, *Exposure of PM2.5 and EC from diesel and gasoline vehicles in communities near the Ports of Los Angeles and Long Beach, California*, Atmos. Environ. **43**, 1962 (2009), doi: 10.1016/j.atmosenv.2009.01.009.

[12] M. C. MacCracken, *Prospects for Future Climate Change and the Reasons for Early Action*, J. Air Waste Manag. Assoc. **58**, 735 (2008), doi: 10.3155/1047-3289.58.6.735.

[13] J. G. Watson, *Visibility: Science and regulation*, J. Air Waste Manag. Assoc. **52**, 628 (2002).

[14] J. C. Chow, J. D. Bachmann, S. S. G. Wierman, and C. V. Mathai, *Visibility: Science and regulation*, J. Air Waste Manag. Assoc. **52**, 973 (2002).

[15] S. Twomey, M. Piepgrass, and T. Wolfe, *An assessment of the impact of pollution on global cloud albedo*, Tellus B **36** (2011).

[16] R. J. Charlson, S. E. Schwartz, J. M. Hales, R. D. Cess, J. A. Coakley, J. E. Hansen, and D. J. Hofmann, *Climate Forcing by Anthropogenic Aerosols*, Science **255**, 423 (1992), doi: 10.1126/science.255.5043.423.

[17] J. E. Penner, R. J. Charlson, S. E. Schwartz, J. M. Hales, N. S. Laulainen, L. Travis, R. Leifer, T. Novakov, J. Ogren, and L. F. Radke, *Quantifying and Minimizing Uncertainty of Climate Forcing by Anthropogenic Aerosols*, Bull. Am. Meteorol. Soc. **75**, 375 (1994).

[18] C. C. Chuang, J. E. Penner, K. E. Taylor, A. S. Grossman, and J. J. Walton, *An assessment of the radiative effects of anthropogenic sulfate*, J. Geophys. Res. Atmos. **102**, 3761 (1997), doi: 10.1029/96JD03087.

[19] S. Solomon, D. Qin, M. Manning, Z. Chen, M. Marquis, K. Averyt, M. Tignor, and H. Miller, *Contribution of Working Group I to the Fourth Assessment Report of the Intergovernmental Panel on Climate Change* (Cambridge University Press).

[20] N. A. of Engineering and N. R. Council, *Energy Futures and Urban Air Pollution: Challenges for China and the United States* (The National Academies Press, Washington, DC), doi: 10.17226/12001.

[21] J. C. Chow, J. G. Watson, D. H. Lowenthal, L.-W. A. Chen, and N. Motallebi, *Black and Organic Carbon Emission Inventories: Review and Application to California*, J. Air Waste Manag. Assoc. **60**, 497 (2010), doi: 10.3155/1047-3289.60.4.497.

[22] World Health Organization regional office for Europe, *Health relevance of particulate matter from various sources* (2007), available at http://www.euro.who.int/__data/assets/pdf_file/0007/78658/E90672.pdf.

[23] K. J. Lane, J. I. Levy, M. K. Scammell, A. P. Patton, J. L. Durant, M. Mwamburi, W. Zamore, and D. Brugge, *Effect of time-activity adjustment on exposure assessment for traffic-related ultrafine particles.*, J Expo Sci Environ Epidemiol **25**, 506 (2015), doi: 10.1038/jes.2015.11.

[24] U.S. Environmental Protection Agency, *Vol. 80, No. 206* (2015), available at https://www.gpo.gov/fdsys/pkg/FR-2015-10-26/pdf/2015-26594.pdf.

[25] Y. Zhang, *Online-coupled meteorology and chemistry models: history, current status, and outlook*, Atmos. Chem. Phys. **8**, 2895 (2008), doi: 10.5194/acp-8-2895-2008.

[26] A. Baklanov, K. Schlünzen, P. Suppan, J. Baldasano, D. Brunner, S. Aksoyoglu, G. Carmichael, J. Douros, J. Flemming, R. Forkel, et al., *Online coupled regional meteorology chemistry models in Europe: Current status and prospects*, Atmos. Chem. Phys. **14**, 317 (2014), doi: 10.5194/acp-14-317-2014.

[27] C. Hogrefe, G. Pouliot, D. Wong, A. Torian, S. Roselle, J. Pleim, and R. Mathur, *Annual application and evaluation of the online coupled WRF-CMAQ system over North America under AQMEII phase 2*, Atmos. Environ. **115**, 683 (2015), doi: 10.1016/j.atmosenv.2014.12.034.

[28] C. Hong, Q. Zhang, Y. Zhang, Y. Tang, D. Tong, and K. He, *Multi-year Downscaling Application of Online Coupled WRF- CMAQ over East Asia for Regional Climate and Air Quality Modeling : Model Evaluation and Aerosol Direct Effects*, Geosci. Model Dev. Discuss. pages 1–37 (2016), doi: 10.5194/gmd-2016-261.

[29] C. M. Gan, J. Pleim, R. Mathur, C. Hogrefe, C. N. Long, J. Xing, D. Wong, R. Gilliam, and C. Wei, *Assessment of long-term WRF-CMAQ simulations for understanding direct aerosol effects on radiation "brightening" in the United States*, Atmos. Chem. Phys. **15**, 12193 (2015), doi: 10.5194/acp-15-12193-2015.

[30] D. C. Wong, J. Pleim, R. Mathur, F. Binkowski, T. Otte, R. Gilliam, G. Pouliot, A. Xiu, J. O. Young, and D. Kang, *WRF-CMAQ two-way coupled system with aerosol feedback: Software development and preliminary results*, Geosci. Model Dev. **5**, 299 (2012), doi: 10.5194/gmd-5-299-2012.

[31] J. Xing, R. Mathur, J. Pleim, C. Hogrefe, C. M. Gan, D. C. Wong, and C. Wei, *Can a coupled meteorology-chemistry model reproduce the historical trend in aerosol direct radiative effects over the Northern Hemisphere?*, Atmos. Chem. Phys. **15**, 9997 (2015), doi: 10.5194/acp-15-9997-2015.

[32] J. Xing, R. Mathur, J. Pleim, C. Hogrefe, C.-M. Gan, D. Wong, C. Wei, and J. Wang, *Air Pollution and climate response to aerosol direct radiative effects: A modeling study of decadal trends across the northern hemisphere*, J. Geophys. Res. Atmos. pages 3510–3532 (2015), doi: 10.1002/2014JD022145.Received.

[33] Y. Zhang, X. Y. Wen, and C. J. Jang, *Simulating chemistry-aerosol-cloud-radiation-climate feedbacks over the continental U.S. using the online-coupled Weather Research Forecasting Model with chemistry (WRF/Chem)*, Atmos. Environ. **44**, 3568 (2010), doi: 10.1016/j.atmosenv.2010.05.056.

[34] J. Fuhrer, L. Skärby, and M. R. Ashmore, *Critical levels for ozone effects on vegetation in Europe*, Environ. Pollut. **97**, 91 (1997), doi: 10.1016/S0269-7491(97)00067-5.

[35] M. Kampa and E. Castanas, *Human health effects of air pollution*, Environ. Pollut. **151**, 362 (2008), doi: 10.1016/j.envpol.2007.06.012.

[36] N. Uysal and R. M. Schapira, *Effects of ozone on lung function and lung diseases.*, Curr. Opin. Pulm. Med. **9**, 144 (2003), doi: 10.1097/00063198-200303000-00009.

[37] I. B. Tager, J. Balmes, F. Lurmann, L. Ngo, S. Alcorn, and N. Kfinzliw, *Chronic Exposure to Ambient Ozone and Lung Function in Young Adults*, Epidemiology **16**, 751 (2013), doi: 10.1097/01.ede.0000183166.68809.bO.

[38] M. Woody, B. Haeng Baek, Z. Adelman, M. Omary, Y. Fat Lam, J. Jason West, and S. Arunachalam, *An assessment of Aviation's contribution to current and future fine particulate matter in the United States*, Atmos. Environ. **45**, 3424 (2011), doi: 10.1016/j.atmosenv.2011.03.041.

[39] J. I. Levy, M. Woody, B. H. Baek, U. Shankar, and S. Arunachalam, *Current and Future Particulate-Matter-Related Mortality Risks in the United States from Aviation Emissions During Landing and Takeoff*, Risk Analysis **32**, 237 (2012), doi: 10.1111/j.1539-6924.2011.01660.x.

[40] D. Byun and J. Ching, *Science Algorithms of the EPA Models-3 Community Multiscale Air Quality (CMAQ) Modeling System*, EPA/600/R-99/030 (1999).

[41] A. M. Dunker, *The decoupled direct method for calculating sensitivity coefficients in chemical kinetics*, J. Chem. Phys. **81**, 2385 (1984), doi: 10.1063/1.447938.

[42] S. L. Napelenok, D. S. Cohan, M. T. Odman, and S. Tonse, *Extension and evaluation of sensitivity analysis capabilities in a photochemical model*, Environ. Model. Softw. **23**, 994 (2008), doi: 10.1016/j.envsoft.2007.11.004.

[43] S. L. Napelenok, D. S. Cohan, Y. Hu, and A. G. Russell, *Decoupled direct 3D sensitivity analysis for particulate matter (DDM-3D / PM)*, Atmos. Environ. **40**, 6112 (2006), doi: 10.1016/j.atmosenv.2006.05.039.

[44] A. Hakami, M. T. Odman, and A. G. Russell, *High-order, direct sensitivity analysis of multidimensional air quality models*, Environ. Sci. Technol. **37**, 2442 (2003), doi: 10.1021/es020677h.

[45] W. Zhang, S. L. Capps, Y. Hu, A. Nenes, S. L. Napelenok, and A. G. Russell, *Model Development Development of the high-order decoupled direct method in three dimensions for particulate matter : enabling advanced sensitivity analysis in air quality models*, Geosci. Model Dev. **5**, 355 (2012), doi: 10.5194/gmd-5-355-2012.

[46] C. Roof and G. G. Fleming, *Aviation Environmental Design Tool (AEDT)*, 22nd Annual UC Symposium on Aviation Noise and Air Quality pages 1–30 (2007).

[47] B. Baek, S. Arunachalam, M. Woody, L. Vennam, M. Omary, F. Binkowski, and G. Fleming, *A New Interface to Model Global Commercial Aircraft Emissions from the FAA Aviation Environmental Design Tool (AEDT) in Air Quality Models*, Presented at the 11th Annual CMAS Conference (2012).

[48] U.S. Environmental Protection Agency, *National Emissions Inventory (NEI)* (2005), available at https://www.epa.gov/air-emissions-inventories/national-emissions-inventory-nei.

[49] M. R. Houyoux, J. M. Vukovich, C. J. Coats, N. J. M. Wheeler, and P. S. Kasibhatla, *Emission inventory development and processing for the Seasonal Model for Regional Air Quality (SMRAQ) project*, J Geophys Res Atmos **105**, 9079 (2000), doi: 10.1029/1999JD900975.

[50] W. Skamarock, J. Klemp, J. Dudhi, D. Gill, D. Barker, M. Duda, X.-Y. Huang, W. Wang, and J. Powers, *A Description of the Advanced Research WRF Version 3*, Technical Report page 113 (2008), doi: 10.5065/D6DZ069T.

[51] M. M. Rienecker, M. J. Suarez, R. Gelaro, R. Todling, J. Bacmeister, E. Liu, M. G. Bosilovich, S. D. Schubert, L. Takacs, G. K. Kim, et al., *MERRA: NASA's modern-era retrospective analysis for research and applications*, J. Climate **24**, 3624 (2011), doi: 10.1175/JCLI-D-11-00015.1.

[52] J. F. Lamarque, L. K. Emmons, P. G. Hess, D. E. Kinnison, S. Tilmes, F. Vitt, C. L. Heald, E. A. Holland, P. H. Lauritzen, J. Neu, et al., *CAM-chem: Description and evaluation of interactive atmospheric chemistry in the Community Earth System Model*, Geosci. Model Dev **5**, 369 (2012), doi: 10.5194/gmd-5-369-2012.

[53] J. Seinfeld and S. Pandis, *Atmospheric Chemistry and Physics* (John Wiley and Sons, New York).

[54] J. R. Kinosian, *Ozone-Precursor Relationships from EKMA Diagrams*, Environ. Sci. Technol. **16**, 880 (1982), doi: 10.1021/es00106a011.

[55] T. Stoeckenius, J. Johnson, and T. Shah, *Addendum to AIR QUALITY MODELING STUDY FOR THE FOUR CORNERS REGION Additional Ozone Source Apportionment and Ozone Sensitivity Modeling Analyses* (2010), available at https://www.env.nm.gov/aqb/4C/Documents/FourCornersModelingAddendum_5April2010.pdf.

[56] D. S. Cohan and S. L. Napelenok, *Air Quality Response Modeling for Decision Support*, Atmosphere **2**, 407 (2011), doi: 10.3390/atmos2030407.

[57] B. Koo, G. M. Wilson, R. E. Morris, A. M. Dunker, and G. Yarwood, *Comparison of Source Apportionment and Sensitivity Analysis in a Particulate Matter Air Quality Model*, Environ. Sci. Technol **43**, 6669 (2009), doi: 10.1021/es9008129.

[58] U.S. Environmental Protection Agency, *Nonattainment Areas for Criteria Pollutants (Green Book)* (2017), available at https://www.epa.gov/green-book.

[59] U.S. Federal Aviation Administration, *List of Commercial Service Airports in the United States and their Nonattainment and Maintenance Status* (2016), available at https://www.faa.gov/airports/environmental/vale/media/vale_eligible_airports.xlsx.